Microporous and Mesoporous Materials 137 (2011) 83–91

Contents lists available at ScienceDirect

Microporous and Mesoporous Materials

journal homepage: www.elsevier.com/locate/micromeso

A molecular dynamics investigation of the diffusion characteristics of cavity-type zeolites with 8-ring windows

Rajamani Krishna [a,b,*], Jasper M. van Baten [a]

[a] Van 't Hoff Institute for Molecular Sciences, University of Amsterdam, Science Park 904, 1098 XH Amsterdam, The Netherlands
[b] Department of Chemical and Biomolecular Engineering, University of California, Berkeley, CA 94720, USA

ARTICLE INFO

Article history:
Received 5 July 2010
Received in revised form 25 August 2010
Accepted 31 August 2010
Available online 7 September 2010

Keywords:
8-Ring windows
Molecular dynamics
Framework flexibility
Zeolites
CO_2 capture

ABSTRACT

Molecular dynamics (MD) simulations are used to investigate the diffusion characteristics in DDR, CHA, LTA, ITQ-29, and TSC zeolites that have cavities separated by 8-member ring windows of dimensions in the 3.4–4.6 Å range. These zeolites have potential usage for separation of a variety of mixtures, such as CO_2/CH_4, CO_2/H_2, H_2/CH_4, and propane/propene, relying on a combination of adsorption and diffusion selectivities. The magnitude of self-diffusivities, $D_{i,self}$, of the CH_4 is found to have a direct correlation with the size of the window opening, increasing by about two orders of magnitude for a 0.5 Å increase in the window aperture. The diffusion selectivities of CO_2/CH_4, and H_2/CH_4 mixtures were also found to have direct, and strong, correlation, with the window aperture. This opens up the possibility of tuning diffusion selectivities by appropriate choice of the framework structure.

Framework flexibility dynamics have also been investigated with the aid of two published force fields for all-silica zeolites. Due to the lattice vibrations there is a distribution of window sizes that varies with time. The diffusivity of CH_4 for a flexible lattice was found to correlate with aperture size of the *time-averaged* window, in precisely the same manner as for fixed framework lattices. This leads to the conclusion that lattice flexibility, *per se*, has no influence on the magnitude of the diffusivity or diffusion selectivity.

1. Introduction

Zeolites such as DDR, CHA, LTA, ITQ-29, and TSC, with 8-ring windows separating adjoining cavities, offer considerable potential for use in separation of mixtures of gases. Potential applications include the separation of mixtures of CO_2/CH_4, CO_2/H_2, H_2/CH_4, and propane/propene [1–17]. The separation principle is based not only on the differences in the adsorption characteristics, but also on the differences in the diffusivities of the guest molecules across the windows that are typically in the 3.4–4.6 Å size range.

Several publications in the published literature have emphasized the important role played by the size of the window on the self-diffusivities, $D_{i,self}$, of guest molecules in cavity-type zeolites [1–3,7,8,18–20]. For each cavity-type zeolite two dimensions of the 8-ring windows can be identified as indicated in Fig. 1: (1) the shortest distance, d_{min}, and (2) the longest distance, d_{max}; these distances are also called "straight" and "diagonal" respectively in the work of Combariza et al. [9]. The values of d_{min}, and d_{max} are obtained by subtracting the van der Waals diameter of O atoms, taken equal to 2.7 Å, from the centre-to-centre distances of framework atoms in the 8-ring windows. The diameters determined following the method of Delaunay triangulation, described in the work by Foster et al. [21] correspond with the d_{min} values; these also represent the maximum hard-sphere diameter that can pass through the 8-ring windows. The PFG NMR experiments of Hedin et al. [8] indicate a difference in the value of $D_{i,self}$ for CH_4 by two orders of magnitude when comparing DDR (d_{min} = 3.65 Å), and ITQ-29 (d_{min} = 4 Å). For any chosen host structure, the diffusivities of different guest molecules can vary by a few orders of magnitude, depending on the degree of constraint at window region. This forms the basis for diffusion-selective separation of propane from propene [1,3,9,20].

In this paper we have used molecular dynamics (MD) to systematically study the importance of window dimensions on the diffusion characteristics of cavity-type zeolites. This article has a set of four objectives.

Firstly, we seek to determine if there is a *direct* correlation between $D_{i,self}$ and the window dimension, d_{min}. This would help set the work of Hedin et al. [8] in a broader perspective.

Secondly, we investigate the influence of the window aperture on the variation of $D_{i,self}$ with the pore concentration, c_i. This aspect has not been given its due attention in the published literature. We aim to show that the size of the window aperture has a direct relation with the steepness with which $D_{i,self}$ increases with increasing c_i.

* Corresponding author at: Van 't Hoff Institute for Molecular Sciences, University of Amsterdam, Science Park 904, 1098 XH Amsterdam, The Netherlands. Tel.: +31 20 6270990; fax: +31 20 5255604.
E-mail address: r.krishna@uva.nl (R. Krishna).

1387-1811/$ - see front matter © 2010 Elsevier Inc. All rights reserved.
doi:10.1016/j.micromeso.2010.08.026

Nomenclature

c_i	concentration of species i, based on accessible pore volume (mol m^{-3})	q_i	molar loading of species i (mol kg^{-1})
c_t	total concentration in mixture (mol m^{-3})	S_{diff}	diffusion selectivity, dimensionless
d_{min}	minimum value of window dimension (m)	V_p	accessible pore volume, (m^3 kg^{-1})
d_{max}	maximum value of window dimension (m)	*Greek letter*	
$D_{i,self}$	self-diffusivity of species i, (m^2 s^{-1})	Γ_i	thermodynamic factor, dimensionless
f_i	fluid phase fugacity of species i (Pa)		

Thirdly, we investigate how the diffusion selectivity, S_{diff}, for a binary mixture defined as the ratio

$$S_{diff} = \frac{D_{1,self}}{D_{2,self}} \quad (1)$$

is related to the window size. The answer to this question is important in deciding the optimal structure to use for diffusion-selective separations.

The fourth objective is to determine whether framework flexibility influences the diffusivities, and S_{diff}. Though there have been several investigations in the published literature on the influence of lattice flexibility on the diffusivity of guest molecules in structures such as LTA, and CHA [9,22–24], much less attention has been paid to its influence on S_{diff}.

For a general background on the molecular simulation techniques used in this work, the reader is referred to Frenkel and Smit [25], Vlugt et al. [26], Dubbeldam and Snurr [27], and Smit and Maesen [28]. The force fields for CH_4, and CO_2 correspond to the ones presented in the works of Dubbeldam et al. [29], and Makrodimitris et al. [30], as presented in the paper by García-Pérez et al. [31] The force field for H_2 corresponds to that given by Kumar et al. [32]. The force fields information for the simulations with cations are taken from Calero et al. [33–36]. In the MD simulations the cations were allowed to move within the framework and both Lennard–Jones and Coulombic interactions are taken into consideration.

The details of the cavity-type zeolite structures investigated (unit cell dimensions, accessible pore volume, characteristic pore dimensions), pore landscapes, detailed specification of the force fields used, simulation methodology, and simulation data on self-diffusivities are available in the Supplementary material accompanying this publication.We begin with an analysis of the diffusion characteristics rigid framework structures.

2. MD simulations of rigid framework structures

Consider the self-diffusivities, $D_{i,self}$, of CH_4 at 500 K, calculated assuming the original crystalline framework to remain rigid. The $D_{i,self}$ are plotted in Fig. 2a as a function of the pore concentration c_i, expressed in terms of the accessible pore volumes, V_p. The pore concentrations, c_i, are obtained by dividing the molar loading q_i, expressed in moles per kg of framework, by the accessible pore volume, i.e. $c_i = q_i/V_p$.

The importance advantages of the use of c_i, instead of molar loadings q_i, has been explained in detail in our earlier work [16,37,38]; its use allows a fairer comparison of the loadings in different microporous structures. For every structure, the accessible pore volume was determined with the aid of molecular simulations using the helium probe insertion technique suggested by Talu and Myers [39,40]. In all the investigated cavity-type zeolites, the molecules jump one-at-a-time across the narrow windows; this is best appreciated by viewing the Video animations 1–7, provided as Supplementary Material in the online version of this Journal. Videos 1 and 2 illustrate the inter-cavity hops of CH_4 in LTA-Si (the all-silica version of LTA zeolite), and DDR respectively. Video 4 is an animation of the motion of CH_4 in LTA-4A, with 96 Na^+ per unit cell. In this case it is clearly observed that the cations (blue colored in the animations) partially block the window regions

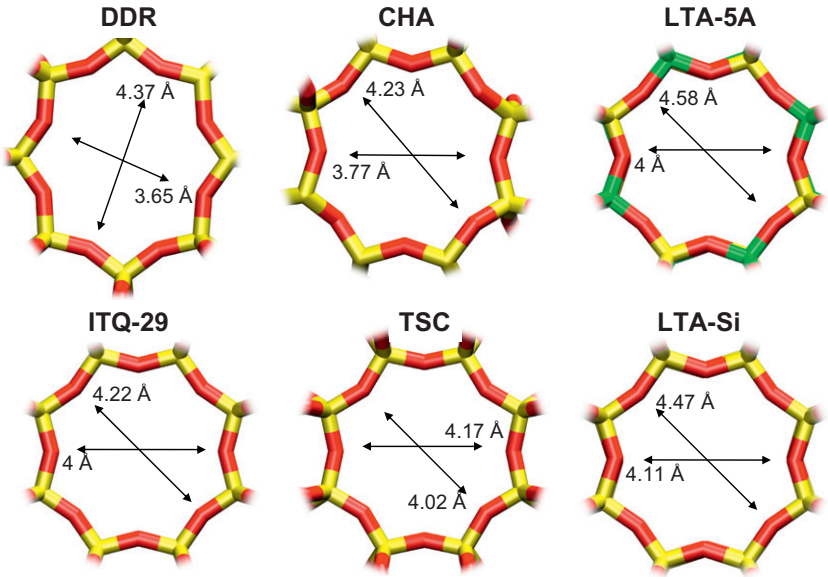

Fig. 1. Window dimensions for cavity-type zeolites DDR, CHA, LTA-5A, ITQ-29, TSC, and LTA-Si. Two dimensions of the 8-ring windows are indicated: (1) the shortest ("straight") distance, d_{min}, and (2) the longest ("diagonal") distance, d_{max}.

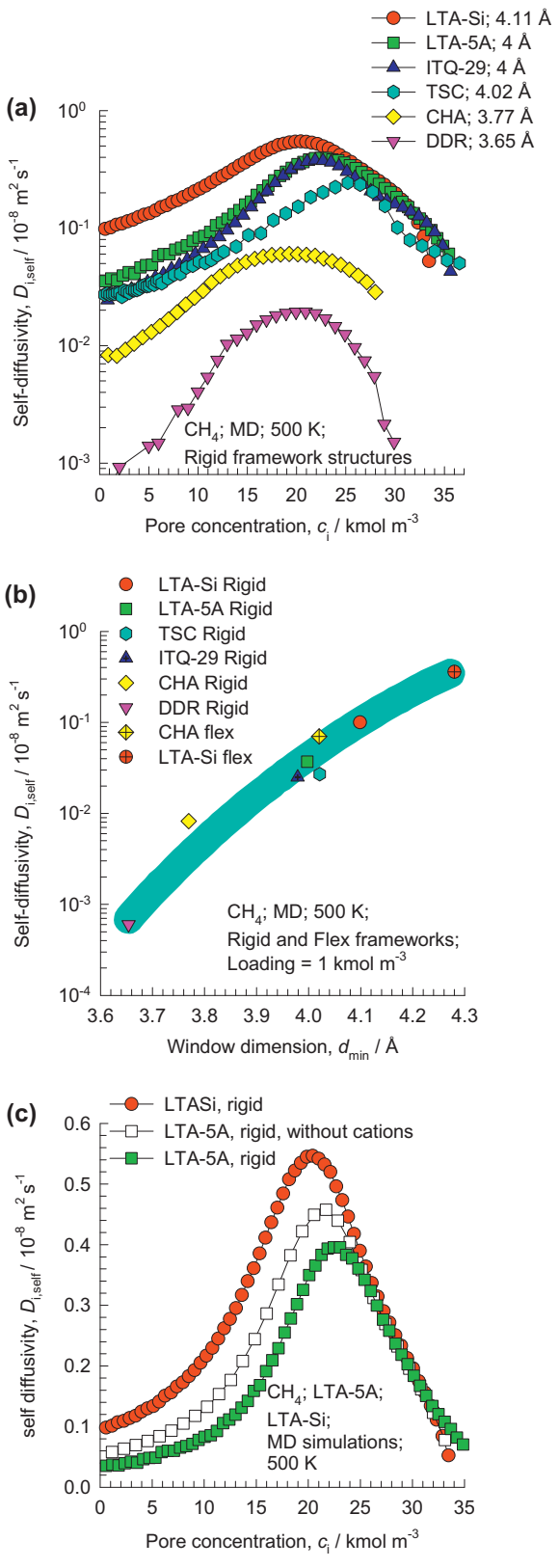

Fig. 2. (a) MD simulations of the self-diffusivities, $D_{i,self}$, of CH_4 in a variety of zeolites at 500 K as a function of the concentration c_i within the pores, expressed in terms of the accessible pore volume. (b) Values of $D_{i,self}$ in (a), determined at a concentration c_i = 1 kmol m^{-3}, plotted as a function of the window dimension d_{min}, as indicated in Fig. 1. For flexible structures the d_{min} values correspond to the first peaks of the probability distributions of the window sizes shown in Fig. 6. (c) MD simulations of the self-diffusivities, $D_{i,self}$, of CH_4 in a LTA-Si, and LTA-5A zeolites at 500 K as a function of the pore concentration.

[35,41]. Consequently, the diffusivities are too low to be determined by MD [38]. For LTA-5A (see Video 3), with 32 Na^+ and 32 Ca^{++} per unit cell, there is no blocking of the windows by the cations [35,42] and the diffusivities are determinable by MD [38].

The hierarchy of diffusivity values follows the hierarchy of d_{min} values, with the highest values for LTA-Si (d_{min} = 4.11 Å), and the lowest for DDR (d_{min} = 3.65 Å). For all structures the $D_{i,self}$ first increases with increasing pore concentration c_i, reaches a maximum, and then decreases on further increase in c_i. The window regions offer high energy barriers for the inter-cavity hopping of guest molecules. The initial increase in the $D_{i,self}$ with c_i is explainable in terms of a reduction in the free-energy barrier for inter-cavity hopping [43,44].

The significance of the window dimension is better illustrated by comparing the self-diffusivity values at a pore concentration value c_i = 1 kmol m^{-3}; see Fig. 2b. Increasing the window aperture, taken to be d_{min}, from 3.65 Å for DDR to 4.11 Å for LTA-Si, results in an increase in $D_{i,self}$ by two orders of magnitude. These MD results are in qualitative agreement with the PFG NMR data presented in Table 1 of Hedin et al. [8]. Kärger [18] has remarked that the diffusivity data of Hedin et al. [8] may not represent genuine intra-crystalline diffusion, and are perhaps influenced by other transport resistances. Consequently, a direct quantitative comparison with MD simulation results is not possible.

A further point that needs examination is the influence of cations. For this purpose we compare in Fig. 2c the $D_{i,self}$ data for LTA-Si (d_{min} = 4.11 Å). with that for LTA-5A (d_{min} = 4 Å; Si/Al = 1; 4 Na^+ and 4 Ca^{++} per cavity). The diffusivities in LTA-5A are lower than in LTA-Si for two separate reasons. To explain these reasons, we also carried out MD simulations using the LTA-5A framework, but without inclusion of any cations; the results are represented by the open square symbols in Fig. 2c. The $D_{i,self}$ data for LTA-5A (without cations) lie below that of LTA-Si, because of the lower d_{min} of the framework; this result is in line with the data presented in Fig. 2b. The $D_{i,self}$ data for LTA-5A (with cations) is also lower than for the same framework in which the cations are excluded. The rationale is that the adsorption strength of CH_4 in LTA-5A is considerably higher due to the interactions with cations; this results in an increasing "sticking" tendency and a lower diffusivity, as explained in detail in our earlier work [38].

A clearer picture of the concentration dependence is obtained by normalizing the $D_{i,self}$, with respect to the zero-concentration value $D_{i,self}(c_i \to 0)$; see Fig. 3a. These data show that the increase in the $D_{i,self}$ in the 5–20 kmol m^{-3} range is sharpest for DDR that has the smallest window aperture. Also, the shallowest increase in the $D_{i,self}$ is for LTA-Si with the largest value of d_{min}. We also note that the largest peak-height in Fig. 3a is for DDR, that has the smallest window aperture, as well as the smallest cavity volume. The guest molecules are in closer proximity within DDR, than in other zeolites, and this could perhaps explain the stronger influence of loading on the free-energy barrier for inter-cavity hopping.

A further point to note from the data presented in Fig. 3a is that the $D_{i,self}$ appear to converge to the same value at a pore concentration of $c_i \approx 35$ kmol m^{-3}. This value corresponds to the saturation capacity of CH_4, as is evidenced by the Configurational-Bias Monte Carlo (CBMC) simulations of the pure component isotherms; see Fig. 3b.

For all cavity-type zeolites investigated, the maximum in the $D_{i,self}$ occurs at a loading that lies intermediate between the first and second inflection points in the isotherm. As illustration, Fig. 3c presents a comparison of $D_{i,self}$ data ITQ-29 with the thermodynamic factor, $\Gamma_i = \partial \ln f_i / \partial \ln c_i$, obtained by analytic differentiation of the isotherm. There are 8 preferred sites within the cavities of ITQ-29; when these are occupied we obtain the first inflection point. At higher loadings the sites near the window regions start to get occupied, and this causes a decrease in the

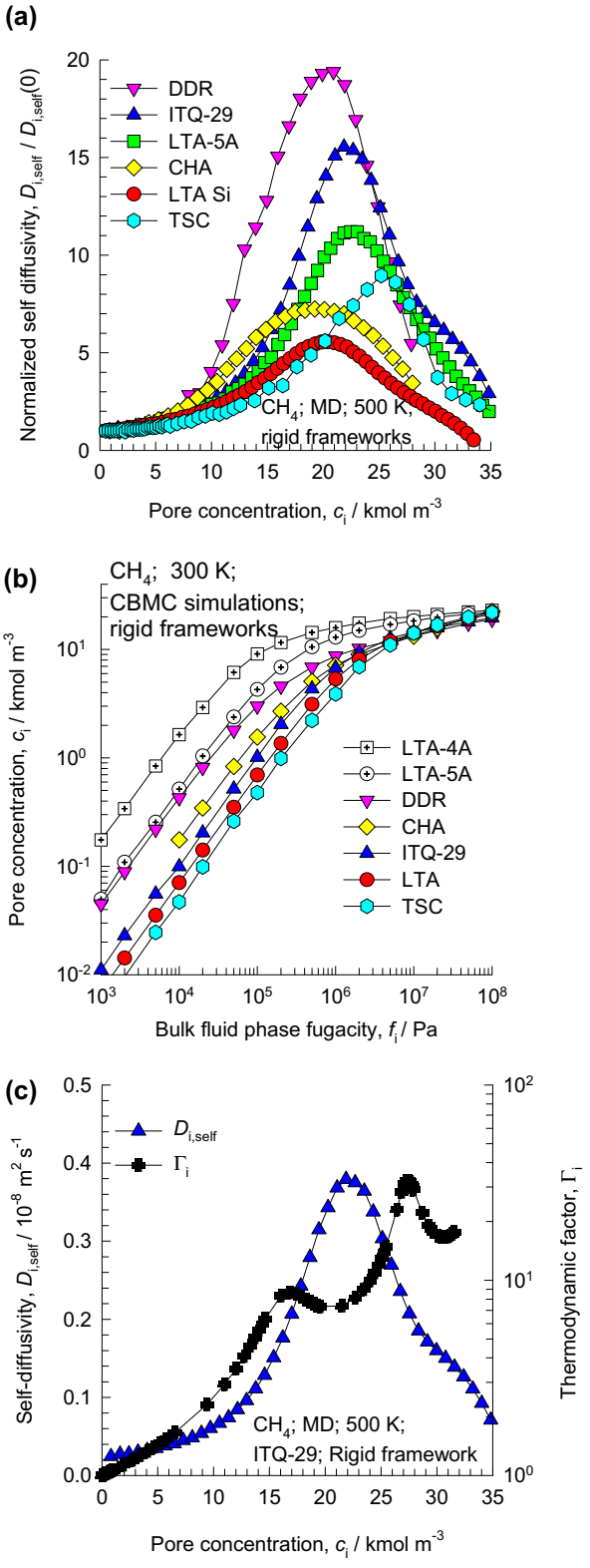

Fig. 3. (a) MD simulations of the self-diffusivities, $D_{i,self}$, normalized with respect to the zero-concentration value $D_{i,self}(0)$, of CH_4 in a variety of zeolites at 500 K. (b) CBMC of the pure component isotherms of CH_4 in a variety of zeolites at 300 K. (c) Comparison of the MD simulations of the self-diffusivities, $D_{i,self}$, in ITQ-29 at 500 K with the thermodynamic factor, $\Gamma_i = \partial \ln f_i / \partial \ln c_i$, obtained by analytic differentiation of the isotherm in (b).

diffusivity values. Data analogous to that shown in Fig. 3c are obtained for all other structures; see Supplementary Material accompanying this publication.

The window dimension also influences the temperature dependence of the diffusivities. Fig. 4 presents Arrhenius plots for the self-diffusivities, $D_{i,self}$, of CH_4 in a variety of zeolites, determined at a concentration $c_i = 2.5$ kmol m^{-3}. We note that the smaller the value of d_{min}, the higher the activation energy. This is a rational result. The stronger the degree of confinement of the guest molecules at the window regions, the stronger the free-energy barrier for inter-cavity hopping, and the higher is the activation energy for diffusion.

The strong dependence of the $D_{i,self}$ of CH_4 on the pore concentration has consequences for the diffusion selectivities on CO_2/CH_4 and H_2/CH_4 mixtures. For both these mixtures, CH_4 is more tightly constrained at the window regions and therefore dependence of the diffusion selectivity S_{diff} on the total mixture concentration, $c_t = c_1 + c_2$, is primarily dictated by the characteristics of the self-diffusivity of CH_4. From the data on S_{diff} for CO_2/CH_4 mixtures shown in Fig. 5a, three things are noteworthy. Firstly, the S_{diff} values exceed unity for all structures because CO_2 molecules jump length-wise across the windows and are less tightly constrained. This is best appreciated by viewing the video animations 8–10. Secondly, the hierarchy of S_{diff} values decreases, by one to two orders of magnitude, with increasing d_{min}. This is because of the increase of the CH_4 diffusivity with increasing d_{min} (cf. Fig. 2b). Thirdly, the rate of decrease of S_{diff} with increasing c_t is higher for structures with smaller window opening. The rationale for the differences in the *rate of decrease* of S_{diff} can be found in differences in the steepness of the initial increase in $D_{i,self}$ of CH_4 as witnessed in Fig. 3a.

The practical implications of the results in Fig. 5a are the following. While, it appears advantageous to choose structures with a smaller window aperture in the interests of increasing S_{diff}, the advantage gets watered down with increased pore loading. Concretely, a comparison of DDR and LTA-Si, shows that S_{diff} is *two orders* of magnitude higher for DDR at $c_t = 1$ kmol m^{-3}. However, at $c_t = 20$ kmol m^{-3}, the S_{diff} advantage of DDR with respect to LTA-Si is reduced to *one order* of magnitude. In practical applications using zeolite membranes for CO_2/CH_4 separation, both S_{diff} and the permeability of the membrane are important. The permeabilities are related to the self-diffusivities $D_{i,self}$. This implies that though DDR will win on S_{diff} considerations, it will lose on the permeability yardstick [16]. A good compromise structure with the

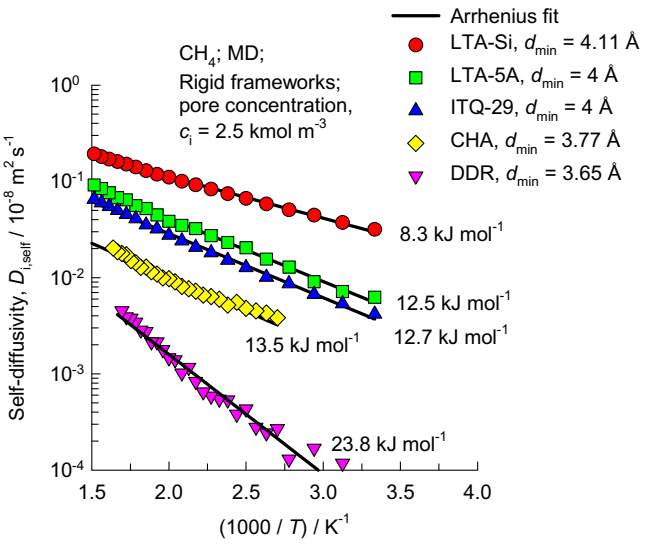

Fig. 4. Arrhenius plots for the self-diffusivities, $D_{i,self}$, of CH_4 in a variety of zeolites, determined at a concentration $c_i = 2.5$ kmol m^{-3}.

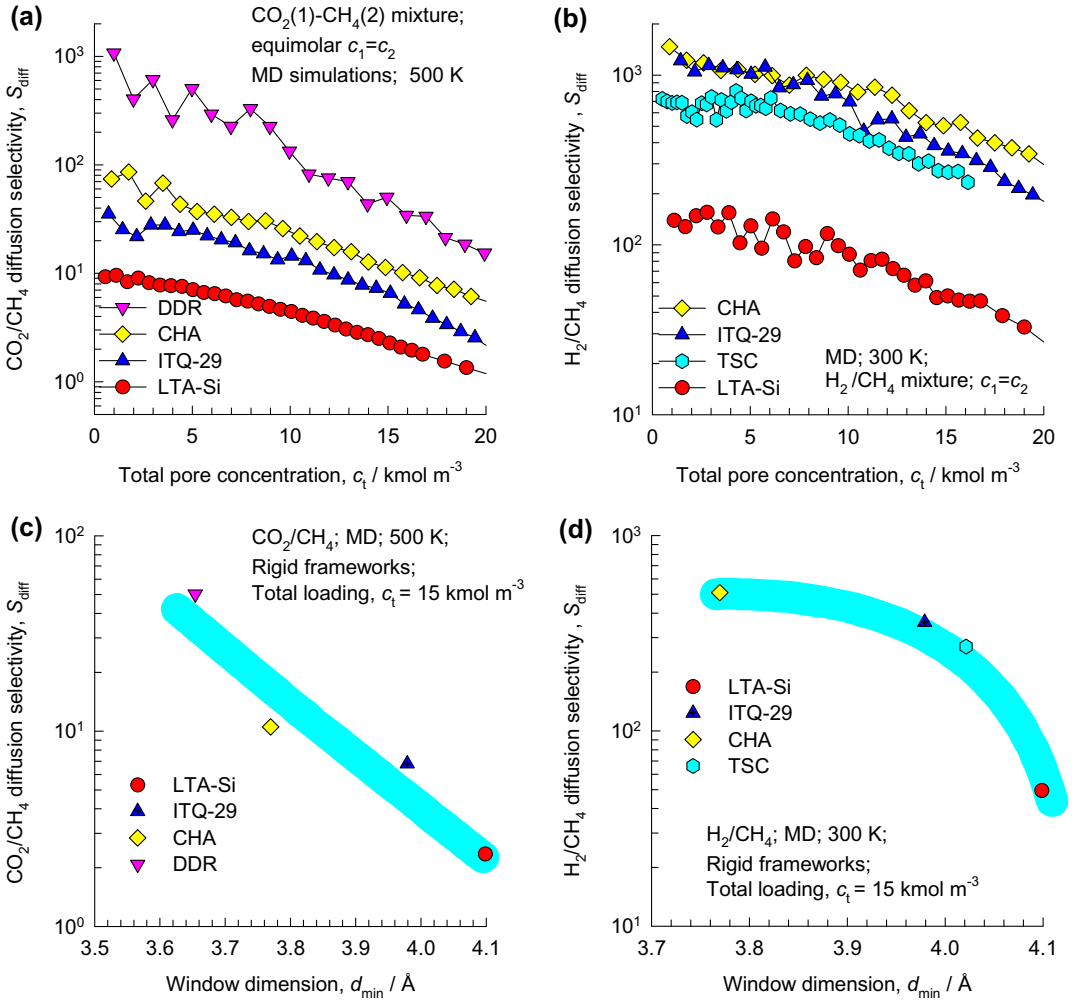

Fig. 5. (a and b) Comparison of diffusion selectivities, S_{diff}, for equimolar ($c_1 = c_2$) (a) CO_2/CH_4, and (b) H_2/CH_4 mixtures in different zeolites, plotted as a function of the total pore concentration $c_t = c_1 + c_2$. (c and d) Diffusion selectivities, S_{diff}, for (c) CO_2/CH_4, (d) H_2/CH_4 mixtures in different zeolites, determined at a total mixture loading $c_t = 15$ kmol m^{-3}, plotted as a function as a function of the window dimension d_{min}.

right combination of selectivity and permeability characteristic could be CHA, as discussed in detail in earlier work [16].

An analogous picture to the above emerges for H_2/CH_4 mixtures; see Fig. 5b. The hierarchy of S_{diff} values is inverse to that of the window opening d_{min}. Again CHA emerges as a good choice for H_2-selective separations.

In Fig. 5c and d, the S_{diff} values at a total mixture loading $c_t = 15$ kmol m^{-3} are plotted as a function as a function of the window dimension d_{min}. For both mixtures, the direct, and strong correlation between S_{diff} and d_{min} is evident.

In the context of the results presented in Fig. 5c, it is important to sound a cautionary note in extrapolating these results to zeolitic imidazolate frameworks (ZIFs). Consider for example the diffusion of CO_2/CH_4 diffusion in ZIF-8; see Video 11. For ZIF-8 that has a SOD topology with windows of 3.4 Å in size, the measurements of Bux et al. [45] for the CO_2/CH_4 diffusion selectivity is about two orders of magnitude lower than that obtained from the extrapolated trends in Fig. 5c. The precise reasons for this needs further detailed investigation.

3. Influence of framework flexibility

Since window openings are so crucially important in determining the diffusion characteristics, the influence of lattice flexibility on diffusivity and diffusion selectivity needs a more detailed attention. The influence of lattice flexibility on diffusion has been the subject of several important papers and reviews [9,22–24,28,46,47]. In order to model the lattice vibrations and framework dynamics we have implemented two different force fields, these force fields are those of: van Beest et al. [48], and Pedone et al. [49]. The implementation of these force fields is carried out in the same manner as described in the paper by Combariza et al. [9] for CHA zeolite, and the simulation methodology do not need to be repeated here. The lattice dynamics for LTA-Si, CHA, and ITQ-29 structures obtained by incorporation of these two force fields can be visualized in Videos animations 12–17.

First, let us consider the influence of framework dynamics on the window dimensions. For the van Beest and Pedone force fields, Fig. 6 presents probability distributions for the window dimensions obtained for flexible framework dynamics of (a) ITQ-29, (b) CHA, and (c) LTA-Si structures; these distributions are obtained without the presence of any guest molecules. The first item of note is that the van Beest and Pedone force fields yield similar distribution functions for window dimensions for all three structures investigated, despite the quite significant differences in flexibility descriptions.

Let us first consider the data in Fig. 6a on window size distributions for ITQ-29, that has a window opening that is practically round, with only a small difference in the values of $d_{min} = 4$ Å, and $d_{max} = 4.22$ Å. Both the van Beest and Pedone force fields for

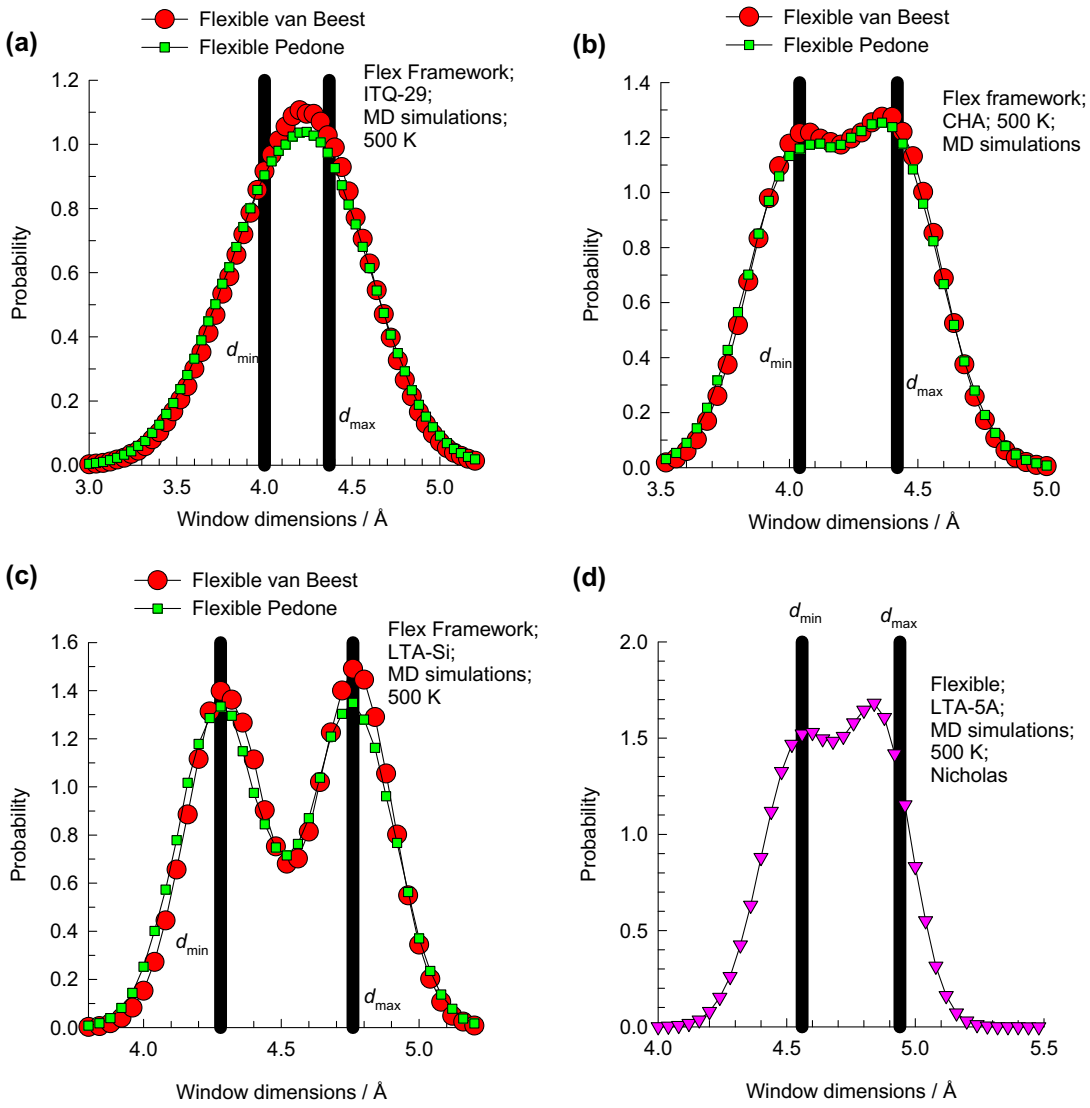

Fig. 6. Distributions of window dimensions obtained for flexible framework dynamics of (a) ITQ-29, (b) CHA, (c) LTA-Si, and (d) LTA-5A. In (a), (b), and (c) the framework dynamics are obtained from MD simulations using the force fields are of van Beest et al. [48], and Pedone et al. [49]; the continuous solid lines indicate the distribution of time-averaged window dimensions using the van Beest force field. In (d) the framework dynamics is obtained from the Nicholas et al. [52] force field.

lattice vibrations yield a similar distribution of window dimensions. From these distributions, the values of the minimum and maximum window dimensions, $d_{min} = 4$ Å, and $d_{max} = 4.37$ Å can be obtained. This suggests that the van Beest and Pedone force fields do not precisely represent the truly crystallographic structure on a time-averaged basis, yielding a larger value of d_{max}. Interestingly, however the value of d_{min} is true to the original crystallographic structure. Since it is the d_{min} that dictates the magnitudes of diffusivity and diffusion selectivity, we should anticipate that the flexibility influences on these parameters would be negligible; we shall return to this point later in the discussions.

The situation is different for CHA, for which the window dimensions for the original rigid frameworks, $d_{min} = 3.77$ Å, and $d_{max} = 4.23$ Å lead to much more asymmetric lattice vibrations. The data in Fig. 6b for the window size distributions for CHA exhibits two peaks; these peaks correspond to minimum and maximum window sizes of 4.04 and 4.42 Å, respectively. Each of these values is significantly higher than that of the original crystallographic structure, $d_{min} = 3.77$ Å, and $d_{max} = 4.23$ Å. The results in Fig. 6b are in agreement with those presented in Figs. 3 and 4 of Combariza et al. [9]. The implication of data in Fig. 6b is that, on a time-averaged basis, the window openings are larger. As discussed in detail by Combariza et al. [9], the van Beest and Pedone force fields also predict a significantly higher unit cell volume than that of the experimentally determined crystallographic structure for CHA. Put another way, neither the van Beest, nor Pedone force fields are truly representative of the native crystallographic structures for CHA. The source of this problem can perhaps be traced to the much stronger asymmetry in the window opening of CHA, as compared to that of the more rounded opening of ITQ-29.

For LTA-Si, the application of the van Beest and Pedone force fields for framework flexibility again leads to two distinct peaks in the window size distributions; see Fig. 6c. The distribution of time-averaged framework atom positions yields two peaks that occur at 4.28 and 4.76 Å; these peaks correspond to minimum and maximum window dimensions. Each of these values is significantly higher than that of the original crystallographic structure, i.e. 4.11 and 4.47 Å. Also for LTA-Si, the van Beest and Pedone force fields do not remain faithful to the original rigid crystallographic structure and yield larger window openings, on a time-averaged basis.

We proceeded to investigate the self-diffusivities of CH_4 in these three structures, taking the framework dynamics into account; the results are summarized in Fig. 7a–c.

Let us first consider self-diffusion of CH_4 in ITQ-29. Fig. 7a shows that the self-diffusivity of CH_4 is practically identical over the entire range of concentrations, irrespective of whether the framework is assumed to be rigid or flexible. The reason for the coincidence of the rigid and flexible structure simulations is that the d_{min} for both is the same, and equal to 4 Å. The choice of the force field, van Beest or Pedone, does not matter either; this is to be expected in view of the almost identical window size distributions shown in Fig. 6a. Another conclusion that can be drawn is that the $D_{i,self}$ is not dependent on the value of d_{max}, that is different for the fixed (4.2 Å) and flexible (4.37 Å) frameworks of ITQ-29.

For both CHA and LTA-Si, for the range of pore concentrations c_i in the range 0–20 kmol m^{-3}, both the van Beest and Pedone force field implementations of flexible framework dynamics show $D_{i,self}$ values that are significantly higher than that of the corresponding, original, rigid crystalline structure; see Fig. 7b and c. The reason for this larger value for the flexible framework can be found in the significantly larger value of d_{min} for both CHA, and LTA-Si, when compared to the rigid crystalline framework. MD simulations were also carried out with a rigid framework, but with the time-averaged framework positions as determined from lattice framework dynamics. For LTA-Si, the diffusivities of flexible and rigid frameworks are the same for loadings $c_i > 25$ kmol m^{-3}; this is because at high loadings intra-cavity hops determine the diffusivity values and the window dimensions are irrelevant. These rigid framework simulations correspond almost exactly with the corresponding fully-flexible MD simulations, underlining the conclusion that framework dynamics, *per se*, have no influence on the self-diffusivities. The higher diffusivity values are entirely ascribable to larger window dimensions in the van Beest and Pedone force field implementations for CHA, and LTA-Si. These conclusions are in complete agreement with those reached by Fritzsche et al. [23,24] for LTA zeolite. Our results also support the conclusion reached in the theoretical study by Kopelevich and Chang [46] that lattice vibrations in zeolites do not drive diffusion.

In a recent paper by García-Sánchez et al. [50], the influence of framework flexibility on the self-diffusivity, $D_{i,self}$, of CH_4 has been investigated in LTA-Si, ITQ-29, and LTA-5A. Two different force fields, those due to Hill and Sauer [51], and Nicholas et al. [52], were used to describe the framework flexibility. These authors did not, however, determine the window size distributions in the manner described in the foregoing. In order to interpret their MD

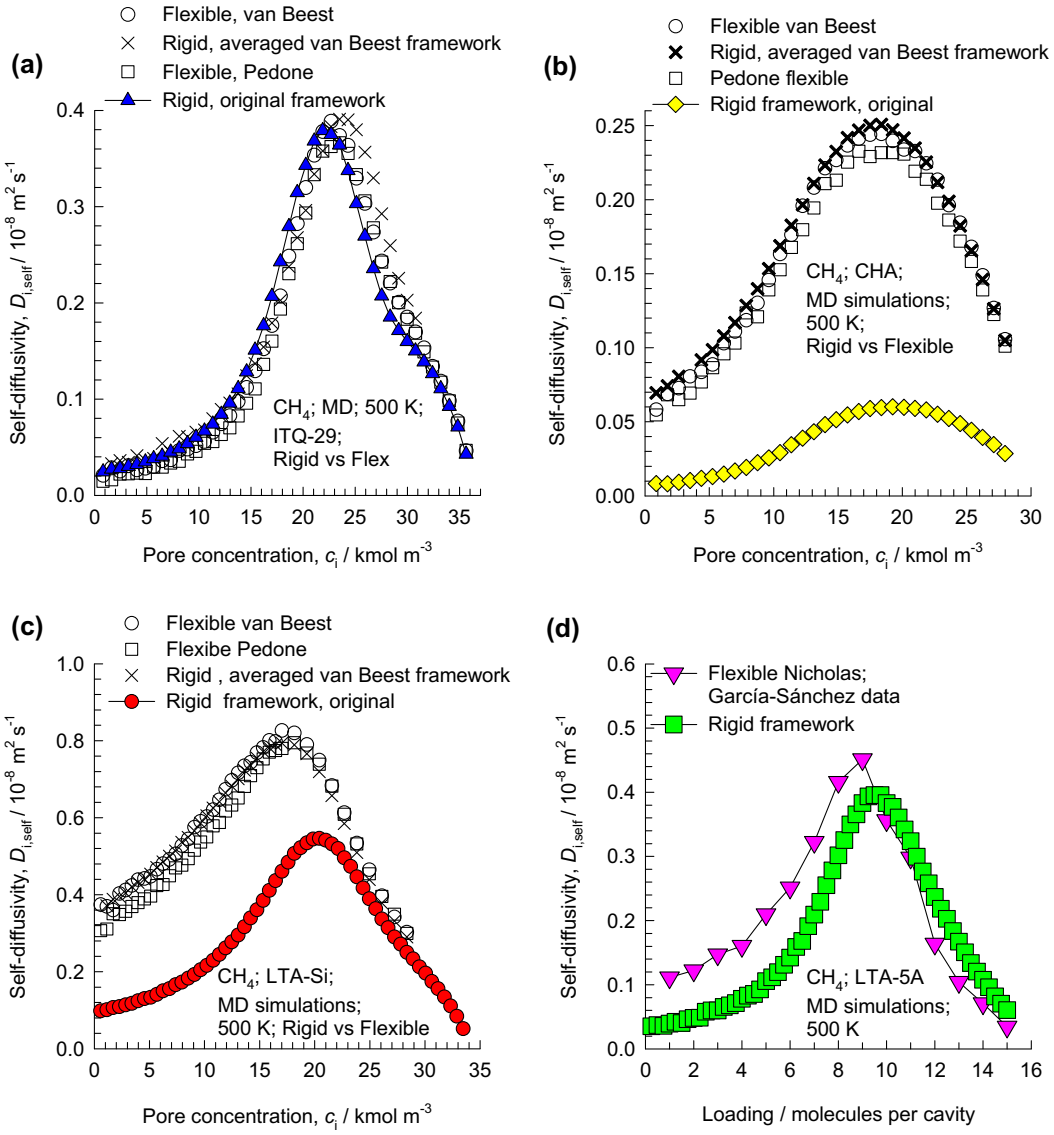

Fig. 7. Comparison of rigid and flexible framework MD simulations of the self-diffusivities, $D_{i,self}$, of CH_4 in (a) ITQ-29, (b) CHA, (c) LTA-Si, and (d) LTA-5A.

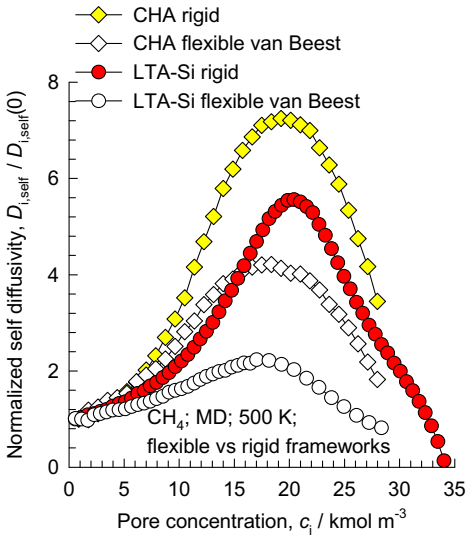

Fig. 8. Comparison of rigid and flexible (van Beest force field) MD simulations of the self-diffusivities, $D_{i,self}$, normalized with respect to the zero-concentration value $D_{i,self}(0)$, of CH_4 in CHA, and LTA-Si.

simulation results in the same manner as described above we determined the corresponding window size distributions in all cases. For illustration purposes, let us consider the window size distributions for LTA-5A using the Nicholas force field implementation; this information is presented in Fig. 6d. The Nicholas force field yields the time-averaged values d_{min} = 4.56 Å, and d_{max} = 4.94 Å. Comparison with the corresponding values for the rigid framework, d_{min} = 4 Å, and d_{max} = 4.58 Å shows that the d_{min} value is higher than that of the rigid framework. We should therefore expect that the MD simulations with a flexible framework using the Nicholas force field to yield higher diffusivity values when compared to the rigid framework; indeed the flexible framework results of García-Sánchez presented in Fig. 7d confirm this expectation. Other flexible framework simulation results of García-Sánchez are amenable to a similar interpretation in terms of the influence of diffusivities on the value of d_{min}; the complete information is provided in the Supplementary Material accompanying this publication.

A different way of emphasizing the fact that lattice vibrations, *per se*, do not influence diffusivities is to include the data for the flexible framework simulations in the plot shown in Fig. 2b. In the extended plot the d_{min} values for the flexible frameworks are obtained from the *first peak* values of the probability distributions in Fig. 6. We note from Fig. 2b that the data on $D_{i,self}$ at a concentration c_i = 1 kmol m^{-3} are uniquely dependent on the appropriately chosen value of d_{min}.

Since the flexible framework simulations yield higher $D_{i,self}$, consonant with higher d_{min} as compared to the original rigid frameworks, we should also expect the initial increases in the $D_{i,self}$ with the pore concentration c_i to be shallower for the flexible frameworks. This is indeed confirmed in the comparisons presented in Fig. 8 of the normalized self-diffusivities for CHA, and LTA-Si.

It must be remarked here that the conclusions regarding the influence of lattice flexibility on diffusion is restricted in its validity to the 8-ring window structures investigated. Flexibility influences in one-dimensional channels of zeolites and metal organic frameworks (MOFs) are of a different nature and significance [47,53,54].

For both CO_2/CH_4, and H_2/CH_4 mixture diffusion in ITQ-29, the diffusion selectivity is practically the same whether the framework is assumed to be rigid or flexible; see the MD simulation results in

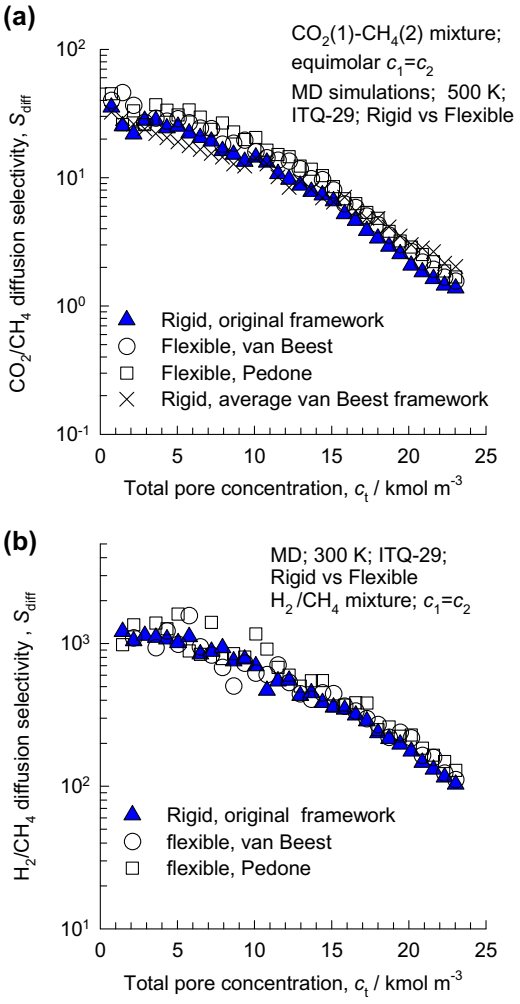

Fig. 9. (a and b) Comparison of diffusion selectivities, S_{diff}, obtained for rigid and flexible lattices, for equimolar (c_1 = c_2) (a) CO_2/CH_4, and (b) H_2/CH_4 mixtures in ITQ-29, plotted as a function of the total pore concentration c_t = c_1 + c_2.

Fig. 9. This implies that the rigid framework simulation, such as those presented in Fig. 5, can be used to selection of the appropriate material for a specific diffusion-selective separation application at hand.

4. Conclusions

On the basis of MD simulations of self-diffusivities $D_{i,self}$, both for unary CH_4 diffusion and for binary mixture diffusion in a variety of cavity-type zeolites, we can draw the following set of conclusions to the four objectives set out in the Section 1.

(1) There is a direct correlation between $D_{i,self}$ and the window dimension, d_{min}. This dependence is depicted in Fig. 2b. The value of d_{max} is not relevant in the determination of the diffusivity of the guest molecules investigated here.
(2) The variation of $D_{i,self}$ with the pore concentration c_i is dictated by d_{min} and is best illustrated by the data presented in Fig. 3a. Broadly speaking, the smaller the value of d_{min}, the sharper is the initial increase of $D_{i,self}$ with c_i. The reason for this is the free-energy barrier for inter-cavity hopping is higher if the guest molecule is more strongly constrained at the window regions.

(3) For CO_2/CH_4 and H_2/CH_4 mixtures, the diffusion selectivity, S_{diff}, is also dictated by d_{min}. The smaller the window aperture, the higher the value of S_{diff}; see Fig. 5.
(4) Lattice dynamics, *per se*, do not appear to influence diffusivities; this conclusion is in line with those already reached in the literature [23,24,46]. This conclusion also applies to the MD simulation results presented by García-Sánchez et al. [50], though the authors themselves did not derive this unequivocal conclusion. Lattice vibrations also have no influence on the diffusion selectivities for mixtures; see Fig. 9.

The results of our investigation will be of help in deciding on the optimum choice of window size to choose for a given separation application.

Acknowledgements

This material is based upon work supported as part of the Center for Gas Separations Relevant to Clean Energy Technologies, an Energy Frontier Research Center funded by the U.S. Department of Energy, Office of Science, Office of Basic Energy Sciences under Award Number DE-SC0001015.

Appendix A. Supplementary data

Supplementary data associated with this article can be found, in the online version, at doi:10.1016/j.micromeso.2010.08.026.

References

[1] P.A. Barrett, T. Boix, M. Puche, D.H. Olson, E. Jordan, H. Koller, M.A. Camblor, Chem. Commun. (2003) 2114–2115.
[2] D.H. Olson, M.A. Camblor, L.A. Vallaescusa, G.H. Kuehl, Microporous Mesoporous Mater. 67 (2004) 27–33.
[3] D.H. Olson, X. Yang, M.A. Camblor, J. Phys. Chem. B 108 (2004) 11044–11048.
[4] J. van den Bergh, W. Zhu, J. Gascon, J.A. Moulijn, F. Kapteijn, J. Membr. Sci. 316 (2008) 35–45.
[5] J. Caro, M. Noack, Microporous Mesoporous Mat. 115 (2008) 215–233.
[6] M. Palomino, A. Corma, F. Rey, Langmuir 26 (2010) 1910–1917.
[7] N. Hedin, G.J. DeMartin, K.G. Strohmaier, S.C. Reyes, Microporous Mesoporous Mater. 98 (2007) 182–188.
[8] N. Hedin, G.J. DeMartin, W.J. Roth, K.G. Strohmaier, S.C. Reyes, Microporous Mesoporous Mater. 109 (2008) 327–334.
[9] A.F. Combariza, G. Sastre, A. Corma, J. Phys. Chem. C 113 (2009) 11246–11253.
[10] M. Palomino, A. Cantin, A. Corma, S. Leiva, F. Rey, S. Valencia, Chem. Commun. (2007) 1233–1235.
[11] S. Li, J.L. Falconer, R.D. Noble, R. Krishna, J. Phys. Chem. C 111 (2007) 5075–5082.
[12] M. Hong, S. Li, J.L. Falconer, R.D. Noble, J. Membr. Sci. 307 (2008) 277–283.
[13] S. Li, M.A. Carreon, Y. Zhang, H.H. Funke, R.D. Noble, J.L. Falconer, J. Membr. Sci. 352 (2010) 7–13.
[14] S. Himeno, T. Tomita, K. Suzuki, K. Nakayama, S. Yoshida, Ind. Eng. Chem. Res. 46 (2007) 6989–6997.
[15] R. Krishna, J.M. van Baten, Chem. Eng. J. 133 (2007) 121–131.
[16] R. Krishna, J.M. Van Baten, J. Membr. Sci. 360 (2010) 323–333.
[17] J. van den Bergh, A. Tihaya, F. Kapteijn, Microporous Mesoporous Mater. 132 (2010) 137–147.
[18] J. Kärger, Microporous Mesoporous Mater. 116 (2008) 715–717.
[19] P. Demontis, L.A. Fenu, G.B. Suffritti, J. Phys. Chem. B 109 (2005) 18081–18087.
[20] D.M. Ruthven, S.C. Reyes, Microporous Mesoporous Mater. 104 (2007) 59–66.
[21] M.D. Foster, I. Rivin, M.M.J. Treacy, O.D. Friedrichs, Microporous Mesoporous Mater. 90 (2006) 32–38.
[22] P. Demontis, G.B. Suffritti, Microporous Mesoporous Mater. 125 (2009) 160–168.
[23] S. Fritzsche, M. Wolfsberg, R. Haberlandt, P. Demontis, G.B. Suffritti, A. Tilocca, Chem. Phys. Lett. 296 (1998) 253–258.
[24] S. Fritzsche, R. Haberlandt, M. Wolfsberg, Chem. Phys. Lett. 253 (2000) 283–294.
[25] D. Frenkel, B. Smit, Understanding Molecular Simulations: From Algorithms to Applications, Academic Press, San Diego, 2002.
[26] T.J.H. Vlugt, J.P.J.M. Van der Eerden, M. Dijkstra, B. Smit, D. Frenkel, Introduction to Molecular Simulation and Statistical Thermodynamics, Universiteit Utrecht, http://www.phys.uu.nl/~vlugt/imsst/, 1 January 2008.
[27] D. Dubbeldam, R.Q. Snurr, Mol. Simulation 33 (2007) 15–30.
[28] B. Smit, T.L.M. Maesen, Chem. Rev. 108 (2008) 4125–4184.
[29] D. Dubbeldam, S. Calero, T.J.H. Vlugt, R. Krishna, T.L.M. Maesen, B. Smit, J. Phys. Chem. B 108 (2004) 12301–12313.
[30] K. Makrodimitris, G.K. Papadopoulos, D.N. Theodorou, J. Phys. Chem. B 105 (2001) 777–788.
[31] E. García-Pérez, J.B. Parra, C.O. Ania, A. García-Sánchez, J.M. Van Baten, R. Krishna, D. Dubbeldam, S. Calero, Adsorption 13 (2007) 469–476.
[32] A.V.A. Kumar, H. Jobic, S.K. Bhatia, J. Phys. Chem. B 110 (2006) 16666–16671.
[33] S. Calero, D. Dubbeldam, R. Krishna, B. Smit, T.J.H. Vlugt, J.F.M. Denayer, J.A. Martens, T.L.M. Maesen, J. Am. Chem. Soc. 126 (2004) 11377–11386.
[34] E. García-Pérez, D. Dubbeldam, T.L.M. Maesen, S. Calero, J. Phys. Chem. B 110 (2006) 23968–23976.
[35] A. García-Sánchez, E. García-Pérez, D. Dubbeldam, R. Krishna, S. Calero, Adsorpt. Sci. Technol. 25 (2007) 417–427.
[36] S. Calero, M.D. Lobato, E. García-Pérez, J.A. Mejías, S. Lago, T.J.H. Vlugt, T.L.M. Maesen, B. Smit, D. Dubbeldam, J. Phys. Chem. B 110 (2006) 5838–5841.
[37] R. Krishna, J.M. van Baten, Chem. Eng. Sci. 64 (2009) 3159–3178.
[38] R. Krishna, J. Phys. Chem. C 113 (2009) 19756–19781.
[39] O. Talu, A.L. Myers, A.I.Ch.E.J. 47 (2001) 1160–1168.
[40] A.L. Myers, P.A. Monson, Langmuir 18 (2002) 10261–10273.
[41] J.J. Pluth, J.V. Smith, J. Am. Chem. Soc. 102 (1980) 4704–4708.
[42] R.L. Firor, K. Seff, J. Am. Chem. Soc. 100 (1978) 3091–3096.
[43] E. Beerdsen, D. Dubbeldam, B. Smit, J. Phys. Chem. B 110 (2006) 22754–22772.
[44] E. Beerdsen, D. Dubbeldam, B. Smit, Phys. Rev. Lett. 96 (2006) 044501.
[45] H. Bux, C. Chmelik, J.M. Van Baten, R. Krishna, J. Caro, Adv. Mater. XXX (2010) XXX–XXX. (http://dx.doi.org/10.1002/adma.201002066).
[46] D.I. Kopelevich, H.C. Chang, J. Chem. Phys. 114 (2001) 3776–3789.
[47] N.E.R. Zimmermann, S. Jakobtorweihen, E. Beerdsen, B. Smit, F.J. Keil, J. Phys. Chem. C 111 (2007) 17370–17381.
[48] B.W.H. van Beest, G.J. Kramer, R.A. van Santen, Phys. Rev. Lett. 64 (1990) 1955–1958.
[49] A. Pedone, G. Malavasi, M.C. Menziani, A.N. Cormack, U. Segre, J. Phys. Chem. B 110 (2006) 11780–11795.
[50] A. García-Sánchez, D. Dubbeldam, S. Calero, J. Phys. Chem. C 114 (2010) 15068–15074.
[51] J.R. Hill, J. Sauer, J. Phys. Chem. 99 (1995) 9536–9550.
[52] J.B. Nicholas, A.J. Hopfinger, F.R. Trouw, L.E. Iton, J. Am. Chem. Soc. 113 (1991) 4792–4800.
[53] K. Seehamart, T. Nanok, J. Kärger, C. Chmelik, R. Krishna, S. Fritzsche, Microporous Mesoporous Mater. 130 (2010) 92–96.
[54] K. Seehamart, T. Nanok, R. Krishna, T. Van Baten, S. Fritzsche, Microporous Mesoporous Mater. 125 (2009) 97–100.